

# Defect-Engineered Ruthenium MOFs as Versatile Heterogeneous Hydrogenation Catalysts

Konstantin Epp,<sup>[a]</sup> Ignacio Luz,<sup>[b, c]</sup> Werner R. Heinz,<sup>[a]</sup> Anastasia Rapeyko,<sup>[b]</sup> Francesc X. Llabrés i Xamena,<sup>\*[b]</sup> and Roland A. Fischer<sup>\*[a]</sup>

Ruthenium MOF  $[\text{Ru}_3(\text{BTC})_2\text{Y}_y] \cdot \text{G}_g$  (BTC = benzene-1,3,5-tricarboxylate; Y = counter ions =  $\text{Cl}^-$ ,  $\text{OH}^-$ ,  $\text{OAc}^-$ ; G = guest molecules = HOAc,  $\text{H}_2\text{O}$ ) is modified *via* a mixed-linker approach, using mixtures of BTC and pyridine-3,5-dicarboxylate (PYDC) linkers, triggering structural defects at the distinct  $\text{Ru}_2$  paddlewheel (PW) nodes. This defect-engineering leads to enhanced catalytic properties due to the formation of partially reduced  $\text{Ru}_2$ -nodes. Application of a hydrogen pre-treatment protocol to the Ru-MOFs, leads to a further boost in catalytic activity. We

study the benefits of (1) defect engineering and (2) hydrogen pre-treatment on the catalytic activity of Ru-MOFs in the *Meerwein-Ponndorf-Verley* reaction and the isomerization of allylic alcohols to saturated ketones. Simple solvent washing could not avoid catalyst deactivation during recycling for the latter reaction, while hydrogen treatment prior to each catalytic run proved to facilitate materials recyclability with constant activity over five runs.

## Introduction

Modifications at the organic linker in metal-organic frameworks (MOFs) allows for both changes in structure, physical properties and chemical reactivity of the materials.<sup>[1]</sup> Concerning the reactivity of MOFs in catalysis, changes of the coordination environment of the secondary building unit (SBU), i.e. free coordination sites at the metal, may drastically influence their catalytic properties.<sup>[2]</sup> A common strategy in creating defective MOFs is to use mixed-linkers in the *de-novo* solvothermal synthesis,<sup>[3,4]</sup> whereby in parallel to the introduction of the regular linker, stoichiometric amounts of a “defect-generating linker” featuring reduced connectivity can be incorporated into the framework by means of a co-polymerization process.<sup>[3]</sup> Thus, unsaturated metal sites are generated, exhibiting diverse

catalytic properties which are not present in the parent frameworks. In our previous work, pyridine-3,5-dicarboxylic acid (PYDC) was incorporated into the Ru analogue of HKUST-1,  $[\text{Ru}_3(\text{BTC})_2\text{Y}_y] \cdot \text{G}_g$  (**1**) (BTC = benzene-1,3,5-tricarboxylate; Y = counter ions =  $\text{Cl}^-$ ,  $\text{OH}^-$ ,  $\text{OAc}^-$ ; G = guest molecules = AcOH,  $\text{H}_2\text{O}$ ) resulting in material  $[\text{Ru}_3(\text{BTC})_{2-x}(\text{PYDC})_x\text{Y}_y] \cdot \text{G}_g$  (**D**).<sup>[5,6]</sup> Therein, the catalytic properties of defect-engineered Ru-MOFs were evaluated in the hydrogenation of olefins, whereas **D** outperformed their untreated parent counterpart **1**. This was explained by the formation of partially reduced Ru-centers (modified PWs) which are undercoordinated due to the incorporation of ditopic carboxylate PYDC linkers (instead of tritopic carboxylates as in the case of BTC) and thus, better accessible showing enhanced catalytic activity when compared to fully coordinated Ru-centers present in the “defect-free” Ru-MOFs (see Figure 1). Interestingly, a pre-treatment protocol involving the exposure of **1** and **D** to hydrogen atmosphere at  $\sim 150^\circ\text{C}$  leads to superior catalytic activity compared to their non-treated analogues.<sup>[7]</sup> *In-situ* UHV-FTIR studies (ultra-high vacuum Fourier transformed infrared spectroscopy), identified Ru-H species at the mixed-valent  $\text{Ru}_2^{\text{II,III}}$  paddlewheels as a key-intermediate, which formation is favored by the defectiveness of the structure present in defect-engineered Ru-MOF. These results broadened our understanding on how defective structure, hydrogen pre-treatment and catalytic reactivity are interlinked and motivated us to study the particular catalytic reactivity of defect-engineered PYDC-containing Ru-MOFs in more detail. Thus, we herein present our investigations regarding the effects of PYDC incorporation into Ru-MOFs on the catalytic activity demonstrated in both the MPV (*Meerwein-Ponndorf-Verley*) reaction and the isomerization of allylic alcohols.

[a] Dr. K. Epp, W. R. Heinz, Prof. R. A. Fischer  
Inorganic and Metal-Organic Chemistry  
Catalysis Research Center and Department of Chemistry  
Technical University of Munich  
Ernst-Otto-Fischer-Straße 1  
D-85748 Garching bei München (Germany)  
E-mail: roland.fischer@tum.de

[b] Dr. I. Luz, A. Rapeyko, Dr. F. X. Llabrés i Xamena  
Instituto de Tecnología Química  
Consejo Superior de Investigaciones Científicas  
Universitat Politècnica de València  
Camí de Vera s/n  
46022 Valencia (Spain)  
E-mail: fllabres@itq.upv.es

[c] Dr. I. Luz  
Current address: RTI International  
Research Triangle Park  
Durham NC-27709-2194 (USA)

Supporting information for this article is available on the WWW under <https://doi.org/10.1002/cctc.201902079>

© 2020 The Authors. Published by Wiley-VCH Verlag GmbH & Co. KGaA. This is an open access article under the terms of the Creative Commons Attribution Non-Commercial NoDerivs License, which permits use and distribution in any medium, provided the original work is properly cited, the use is non-commercial and no modifications or adaptations are made.

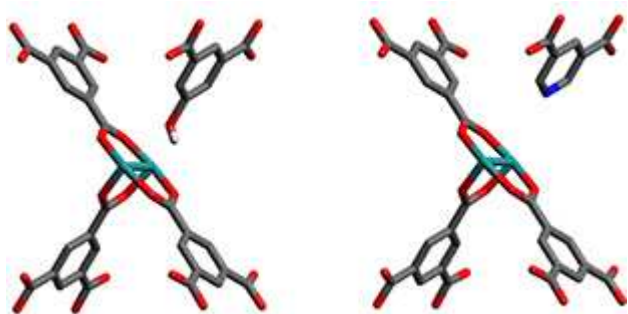


**Figure 1.** Illustration of an ideal Ru paddlewheel (left) ligated by trimesate molecules, compared to a defect-engineered Ru paddlewheel (modified PW) with incorporated PYDC as defect-generating linker (Ru: teal, O: red, N: blue, C: grey, H was omitted for clarity).

## Results and Discussion

### Synthesis and Characterization

In accordance to our previous synthetic protocols, in this study we synthesized defect-engineered Ru–MOF **D30** with a 30% PYDC feeding ratio.<sup>[6]</sup> The incorporation of PYDC was verified by <sup>1</sup>H NMR of acid digested samples (supporting information, S1) in combination with elemental analysis (supporting information, S2).

Due to the fact that no *N*-containing solvent or reagents were used in the synthesis, the *N*-content found in the samples can be associated with the incorporated PYDC. Both data are in good agreement to the suggested sum formula of **D30**  $[\text{Ru}_3(\text{BTC})_{1.4}(\text{pydc})_{0.6}\text{Cl}_x] \cdot \text{AcOH}_{2.65x}$ , showing that slightly less PYDC than the feeding ratio was incorporated in the final solid. **D30** sample is isorecticular to parent Ru–MOF, as it is indicated by powder X-ray diffraction (PXRD) (see supporting information, S3). Moreover, the structural integrity is not significantly affected by the doping, showing the tolerance of the framework to the incorporation of PYDC. Microporous **D30** sample shows a type I isotherm (see supporting information, S4) with BET (Brunauer, Emmett, Teller) surface area of 647 m<sup>2</sup>/g. The thermal stability was investigated by thermal gravimetric analysis (TGA), indicating moderate thermal stability of the defect-engineered sample up to ~220 °C, which is in the same region as their “defect free” parent analogue **1** (see supporting information, S5). **D30** reveals an additional decomposition event which is close to the decomposition temperature of BTC (~220 °C). Most likely, this decomposition step can be associated with the decomposition of PYDC, since both compounds have similar decomposition temperatures. Based on the data obtained by TGA, a BTC to PYDC ratio of 3:1 can be calculated which is in good agreement with the feeding ratios and elemental analysis, giving evidence of the successful incorporation of PYDC. As a crucial procedure to trigger the hydrogenation reactivity of **D30**, the sample was treated with molecular H<sub>2</sub> at elevated temperatures (150 °C), which leads to the desired formation of Ru–H, as previously reported by our group.<sup>[6]</sup> Following on from this interesting catalytic behavior, we tested parent and defect-

engineered Ru–MOFs in two kinds of heterogeneously transition-metal-catalyzed hydrogen-transfer reactions, namely the reduction of carbonyl compounds to alcohols with secondary alcohols as the hydrogen donor (MPV, *Meerwein-Ponndorf-Verley* reaction) and the isomerization of allylic alcohols to saturated ketones. Herein, we want to highlight the H<sub>2</sub> pre-treatment as a key tool of post-synthetic modification of the underlying Ru–MOFs/PYDC-DEMOFs and that the reactivity of PYDC-DEMOFs can be transferred also to other reactions types.

### Catalytic tests

#### Hydrogen transfer reactions

Firstly, we investigated Ru–MOFs in the MPV reaction of cyclohexanone to give cyclohexanol, whereby 2-butanol acts as a hydrogen donor source which formally transfers hydrogen to the unsaturated substrate (ketone). In a typical reaction 10 mg of ketone (0.1 mmol), 5 mg of Ru–MOF catalyst (17 mol% of Ru), and 1 mL of alcohol (ca. 11 eq) were placed into a closed pressured reactor under 2 bar of N<sub>2</sub> at 120 °C. In all the reactions described below, cyclohexanol was the only product detected. Therefore, full selectivity was observed in all cases. Figure 2 shows the time-yield plots obtained for **D30** (30% PYDC) and “defect free” **1** Ru–MOF compounds, both before and after H<sub>2</sub> pre-treatment at 150 °C. The resulting data reveal the higher catalytic activity for **D30** (30% PYDC) compared to **1** the “defect free” Ru–MOF counterpart, providing evidence of the beneficial contribution of the incorporated PYDC defects on the catalytic activity of the system. In particular, the yield when **D30** is used as a catalyst increases from 16 to 43% compared to parent MOF **1** after 2.5 h reaction time.

H<sub>2</sub> pre-treatment causes a further positive impact on the catalytic activity of parent as well as defective Ru–MOFs. The

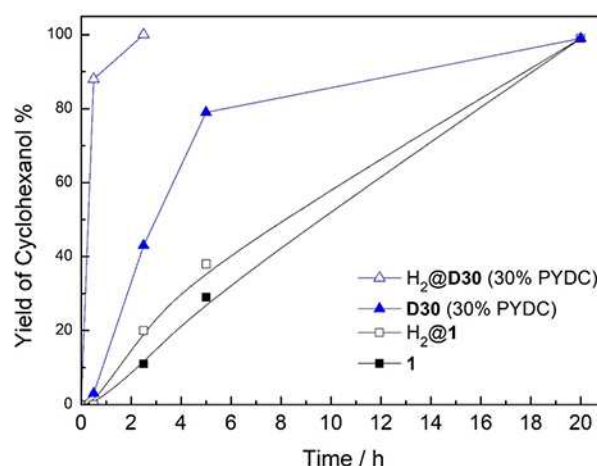
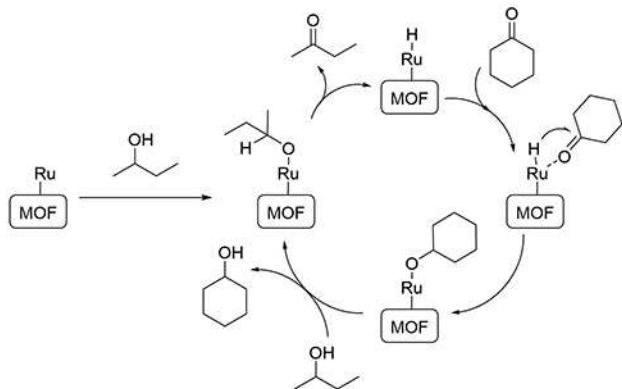


**Figure 2.** Time-yield plot of MPV reaction. Comparison of the reactivity of Ru–MOF/PYDC DEMOF (closed symbols) and their H<sub>2</sub> pre-treated analogues (open symbols). The number in the brackets indicate the feeding ratios of PYDC into parent Ru–MOF.

boost in catalytic activity is much more pronounced in  $H_2@D30$  (hydrogen pre-treated **D30**) reaching 99% yield after 2.5 h the non-treated analog **D30**. Due to introduced point defects like "missing linker", "missing node" and modified PW within the framework of **D30**, the probability of  $H_2$  to access  $Ru_2$ -nodes should be higher than for "defect free"  $Ru$ -MOFs, where only modulator-induced defects are present.<sup>[8]</sup> Therefore, the formation of  $Ru-H$  species is supposed to be more likely. Based on the drastic improvement of the activity of the  $H_2$  pre-treated samples, the reaction mechanism shown in Scheme 1 can be assumed, usually referred to as "hydridic route".<sup>[9]</sup> Unlike classical MPV reactions promoted by aluminum and other non-transition metals involving a direct hydrogen transfer from the alcohol to the ketone via a cyclic transition state, the hydridic route implies the active participation of  $Ru-H$  species similar to other hydride-catalyzed reactions like the dimerization of olefins.<sup>[7]</sup> According to this reaction mechanism, a catalytically active ruthenium hydride species,  $Ru-H$ , is initially formed by the abstraction of the  $\alpha$ -hydrogen of 2-butanol, followed by the MPV-type reduction of cyclohexanone to cyclohexanol. It is thus evident that  $H_2$ -pretreated  $Ru$ -MOFs will show a higher catalytic activity as compared to the corresponding non-treated compounds, since we already demonstrated that  $Ru-H$  species are indeed formed during  $H_2$  pretreatment.<sup>[6]</sup>

A number of ruthenium complexes are well known to catalyze hydrogen transfer reactions,<sup>[9]</sup> and their activity can be significantly boosted by the addition of a small amount of base.<sup>[10]</sup> Note in this sense that the PYDC linkers present in **D30** offer a basic pyridyl-N atom in the proximity of the reactive  $Ru$  centers which may have a similar enhancing effect as an added external base. This would easily explain the large difference in catalytic activity observed for compounds **1** and **D30** (see Figure 2). Secondly, it was investigated if the presented  $Ru-H$  chemistry of PYDC-DEMOFs is transferable to other related reactions, namely the transfer hydrogenation of allylic alcohols to the corresponding saturated ketones. Conversion of allylic alcohols into saturated ketones is usually carried out in two steps: hydrogenation of the  $C=C$  bonds followed by dehydrogenation of the alcohol, which usually requires further protection and deprotection steps. Thus, the one-pot redox

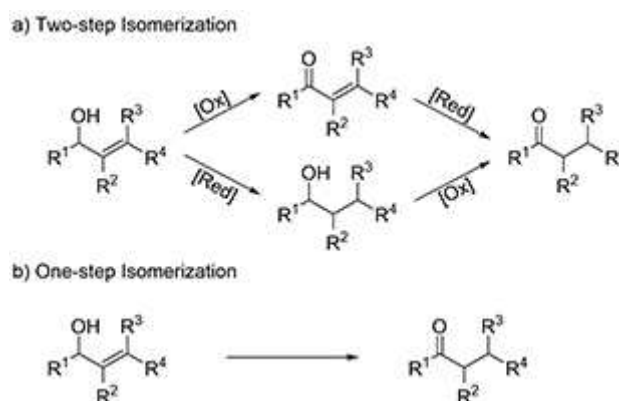


**Scheme 1.** Proposed reaction mechanism for the MPV reduction of cyclohexanone through a "hydridic route".

isomerization evaluated here represents an attractive alternative (see Scheme 2).<sup>[11]</sup>

This reaction can be considered as an intramolecular hydrogen transfer reaction, in which hydrogen is transferred from the alcohol to the  $C=C$  bond. Isomerization of allylic alcohols is usually carried out in the presence of additives, such as bases or hydrogen acceptors, to promote the reaction. Various metals from groups 8, 9, and 10 (including  $Ru$ ) are known to catalyze this reaction.<sup>[12]</sup> As a model reaction to evaluate the activity of  $Ru$ -MOFs, we studied the isomerization of 1-octene-3-ol to octane-3-one in the presence of 2-propanol acting as a solvent as well as a hydrogen donor. In a typical reaction, 40 mg of the allylic alcohol (1-octene-3-ol, ca. 0.3 mmol) 2 mg of  $Ru$ -MOF catalyst (2 mol% of  $Ru$ ), and 1 mL of *i*-PrOH (ca. 13 eq) were placed into a closed pressured reactor under 2 bar of  $N_2$  at 120 °C. The results obtained are shown in Figure 3.

Similar to what was observed in the MPV reaction, both, the introduction of defect-generating PYDC linkers as well as the  $H_2$  pre-treatment result in superior catalytic activity compared to defect-free and non-treated parent  $Ru$ -MOFs (Figure 3). Defect-



**Scheme 2.** a) Two step and b) one step isomerization of allylic alcohols.

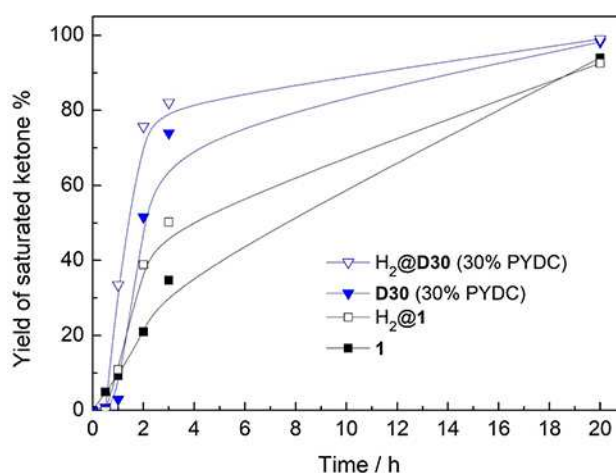
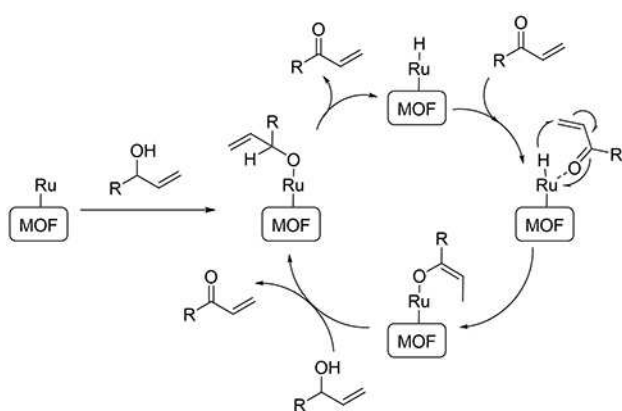


**Figure 3.** Yield-time plot of catalytic transfer hydrogenation of 1-octene-3-ol to octane-3-one using different  $Ru$  catalysts. Comparison between the reactivity of  $Ru$ -MOF/PYDC DEMOF (closed symbols) and their  $H_2$  pre-treated analogues (open symbols).

engineering boosted the catalytic activity of parent Ru–MOF **1** by a factor of about 2.5, namely, from 21 to 52% (**D30**) after 2 h reaction time. Upon H<sub>2</sub> pre-treatment, we observed a 1.9-fold increase in yield (after 2 h reaction time) for **1** (yield increased from 21% to 39%) and by a factor of 1.4 for **D30** (yield from 52% to 75%), respectively. Hence, both strategies for catalyst optimization exhibit a cumulative increase by a factor of roughly 3.6. As it was discussed in the MPV reaction, the higher catalytic activity of the H<sub>2</sub> pre-treated samples and DEMOFs can possibly be explained by the higher amount of incorporated structural point defects resulting in a preferential formation of Ru–H species reasoned by the lower coordination number at the Ru-nodes. As already mentioned above for the MPV reaction, the formation of ruthenium hydride species is a key step in the transfer hydrogenation reaction leading to the isomerization of allylic alcohols to the corresponding saturated ketone. In analogy to the previous report by Yamaguchi *et al.* using Ru(OH)<sub>x</sub>/Al<sub>2</sub>O<sub>3</sub> as a heterogeneous catalyst,<sup>[13]</sup> the overall mechanism for the allylic alcohol isomerization is depicted in Scheme 3. According to the above mechanism, adsorption of the allylic alcohol onto the Ru sites first gives rise to the corresponding alcoholate, followed by the formation of the Ru–H hydride key species and  $\alpha,\beta$ -unsaturated ketone. Then, hydride transfer to the unsaturated ketone gives rise to the corresponding enolate, which is finally desorbed as the saturated ketone upon adsorption of a new allylic alcohol molecule. In order to verify the heterogeneous nature of the catalyst, and to exclude leaching of Ru-species, a hot filtration test has been conducted at low conversion rates showing no further reaction progress as soon as the catalyst was filtered off (see supporting information, S6).

### Recyclability

We selected the isomerization of the allylic alcohol 1-octene-3-ol as a test reaction to evaluate the stability and reusability of the catalysts. To this end, the reaction was first carried out for 2 h following the same procedure as described above. At this



**Scheme 3.** Reaction mechanism for the isomerization of allylic alcohols to saturated ketones over Ru–MOFs.

point, the catalysts were recovered by filtration, thoroughly washed with 2-butanol and dried at room temperature. Catalysts **1** and **D30** were directly used on consecutive catalytic cycles, while H<sub>2</sub> pre-treated catalysts H<sub>2</sub>@**1** and H<sub>2</sub>@**D30** were submitted again to a hydrogenation treatment with H<sub>2</sub> at 150 °C prior to use. The results obtained for five consecutive catalytic cycles are shown in Figure 4. As can be seen, the catalytic activity (*viz.*, yield of saturated ketone obtained after 2 h of reaction) decreases progressively with the use in the case of catalysts **1** and **D30**. This is most likely due to the progressive accumulation of adsorbed species on the solid catalyst like products from previous runs that are not completely removed during washing. This results in an increasing poisoning of the catalytically active sites. Thus, an almost complete loss of activity of the catalysts is observed after already three catalytic cycles. Conversely, catalysts deactivation is not observed for the H<sub>2</sub> pre-treated catalysts H<sub>2</sub>@**1** and H<sub>2</sub>@**D30**. This H<sub>2</sub> pre-treatment of the catalyst between two consecutive catalytic cycles proves to be more effective to remove adsorbed species than solvent washing alone, which most likely explains the preservation of the catalytic activity of these catalysts for at least five consecutive catalytic cycles. Powder X-ray diffraction measurements and TEM images of the collected solids indicate preserved crystallinity (see supporting information Figure S8–9) and particle morphology and size.

### Conclusions

In summary, we demonstrate defect-engineering as an effective synthetic tool for the introduction of structural point defects into ruthenium MOFs and highlight their superior catalytic activity compared to their parent analogues. Additionally, we show that a hydrogen pre-treatment procedure has a strong impact to further boost the catalytic activity of Ru–MOFs which we demonstrated in the MPV reaction (*Meerwein-Ponndorf-*

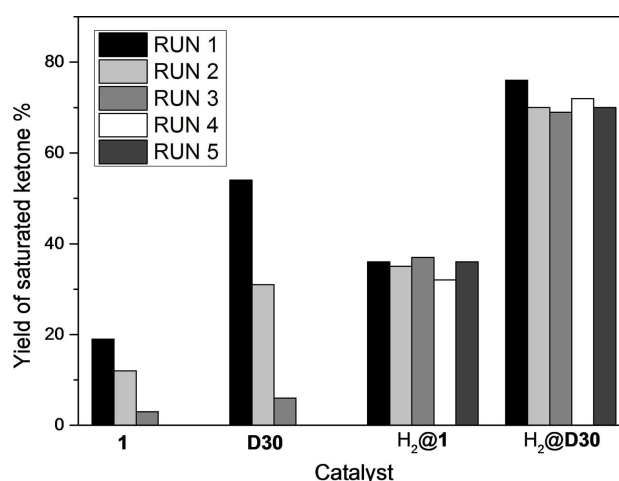


**Figure 4.** Recyclability tests of the Ru–BTC catalysts, showing the yield of saturated ketone obtained after 2 h of reaction with solvent wash (**1** and **D30**) or repeated activation via H<sub>2</sub> pre-treatment (H<sub>2</sub>@**1** and H<sub>2</sub>@**D30**).

Verley) and the isomerization of allylic alcohols. A similar beneficial effect of the hydrogen pretreatment of the Ru–MOFs was already described for the dimerization of ethylene by Agirrezabal-Telleria *et al.* and the hydrogenation of olefins in our previous report.<sup>[6,7]</sup> Moreover, the presence of a basic pyridyl-N atom in the PYDC linkers allowed us to carry out the hydrogen transfer reactions under base free conditions with excellent results and given recyclability.

## Experimental Section

### Materials and Synthesis

RuCl<sub>3</sub>·xH<sub>2</sub>O, LiCl, benzene-1,3,5-tricarboxylic acid (H<sub>3</sub>BTC), and pyridine-3,5-dicarboxylic acid (PYDC) and all solvents [CH<sub>3</sub>COOH, H<sub>2</sub>O, CH<sub>3</sub>OH, acetic anhydride, acetone, hexane, tetrahydrofuran, toluene, EtOH, acetonitrile and MeOH] were used as commercially received unless otherwise noted.

### Synthesis

#### [Ru<sub>2</sub>(OOCCH<sub>3</sub>)<sub>4</sub>Cl]

Tetraaceto-diruthenium (+II, +III) chloride was synthesized following a slightly modified synthesis description which was introduced by Mitchell *et al.*<sup>[14]</sup> 0.5 g RuCl<sub>3</sub>·xH<sub>2</sub>O (~2.4 mmol), 0.5 g LiCl (12 mmol) and 3.5 mL acetic anhydride was mixed with 17.5 mL acetic acid (99.5%) in a 50 mL preheated Schlenk flask. The reaction mixture was stirred and refluxed for 24 h at 140 °C in argon atmosphere. The black suspension turns brown/red after a few hours. Afterwards, it was allowed to cool down to room temperature and the precipitated brown/red solid was filtered (membrane filter) and washed manually using 3×acetone (≥99.8%). Yield: 0.35 g (62%). <sup>1</sup>H NMR δ (298 K, 200 MHz, DMSO-d<sub>6</sub>) 1.9 (s, 3H, –CH<sub>3</sub>) ppm.

#### RuMOF, [Ru<sub>3</sub>(BTC)<sub>2</sub>Y<sub>y</sub>]·G<sub>g</sub> (1)

0.17 g Ru<sub>2</sub>(OOCCH<sub>3</sub>)<sub>4</sub>Cl (1.5 eq.; 0.36 mmol) and 0.1 g H<sub>3</sub>BTC (benzene-1,3,5-tricarboxylic acid) (2 eq.; 0.48 mmol) were dispersed in 4 mL H<sub>2</sub>O (HPLC grade) and 0.7 mL glacial acetic acid, transferred to a PTFE vessel, which was sealed with a stainless steel autoclave and placed in a preheated oven at 150 °C for 72 h. No temperature-controlled program was applied. The reaction mixture was allowed to cool down to r.t. and the liquid was separated from the solid by centrifugation (7830 rpm, 15–20 min). The suspension was decanted and sonicated for 10 min and washed twice with ~20 mL H<sub>2</sub>O (HPLC grade) and acetone with subsequent centrifugation (7830 rpm, 15–20 min). The dark brown solid was dried in vacuum (~10<sup>-3</sup> mbar) and was digested in 4 droplets DCl and around 0.5 mL DMSO-d<sub>6</sub> for <sup>1</sup>H NMR measurement. <sup>1</sup>H NMR δ (298 K, 200 MHz, DMSO-d<sub>6</sub>) 8.6 (s, 3H, C–H<sub>Ar</sub>) ppm, 1.9 (s, 3H, –CH<sub>3</sub>).

#### [Ru<sub>3</sub>(BTC)<sub>2-x</sub>(PYDC)<sub>x</sub>Y<sub>y</sub>]·G<sub>g</sub> (D30)

The defect-engineered Ru–MOF was synthesized in accordance to the synthesis for the parent Ru–MOF, besides adding specific amounts of pyridine-3,5-dicarboxylic acid (PYDC) into the reaction solution. In the synthesis of **D30**, 1.4 eq. of H<sub>3</sub>BTC (71 mg, 0.34 mmol) and 0.6 eq. PYDC (24 mg, 0.14 mmol) were dispersed in 4 mL H<sub>2</sub>O (HPLC grade) and 0.7 mL glacial acetic acid. Afterwards, the mixture was transferred to a PTFE vessel, which was sealed with

a stainless steel autoclave and placed in a preheated oven at 150 °C for 72 h. No temperature-controlled program was applied. The reaction mixture was allowed to cool down to r.t. and the liquid was separated from the solid by centrifugation (7830 rpm, 15–20 min). The suspension was decanted and sonicated for 10 min and washed twice with ~20 mL H<sub>2</sub>O (HPLC grade) and acetone with subsequently centrifugation (7830 rpm, 15–20 min). The black solid was dried in vacuum (~10<sup>-3</sup> mbar) and was digested in 4 droplets DCl and around 0.5 mL DMSO-d<sub>6</sub> for <sup>1</sup>H NMR measurement. <sup>1</sup>H NMR δ (298 K, 200 MHz, DMSO-d<sub>6</sub>) 8.6 (s, 3H, C–H<sub>Ar</sub>) ppm, 1.9 (s, 3H, –CH<sub>3</sub>).<sup>[6]</sup>

### Thermogravimetric analysis (TGA)

Thermogravimetric studies were conducted using a Mettler Toledo TGA/SDTA851e apparatus with an applied heating ramp of 10 °K/min under oxidizing conditions in a N<sub>2</sub>/O<sub>2</sub> (80/20%) flow in Al<sub>2</sub>O<sub>3</sub> crucibles.

### Powder X-ray diffraction (PXRD)

Measurements were performed using Bragg-Brentano geometry on a PANalytical CUBIX diffractometer equipped with a PANalytical X'Celerator detector. X-ray Cu Kα radiation (λ<sub>1</sub> = 1.5406 Å, λ<sub>2</sub> = 1.5444 Å, I<sub>2</sub>/I<sub>1</sub> = 0.5) was used for the measurements. Voltage and intensity were 45 kV and 40 mA, respectively. The arm goniometer length was 200 mm, and a variable divergence slit (irradiated area = 2.5 mm) was employed. The measurement range was from 2.0° to 90.0° (2θ), with a step size of 0.040° (2θ) and an acquisition time of 35 seconds per step. The measurement was performed at 298 K, and the sample was rotated during the measurement at 0.5 rps.

### N<sub>2</sub>-physisorption (BET)

N<sub>2</sub>-physisorption measurements were performed on a Micromeritics ASAP 20120 device using N<sub>2</sub> at 77 K. Before the measurement the samples (~100 mg) were degassed for 12 h at 120 °C under dynamic vacuum.

### Gas Chromatography (GC)

Gas chromatography measurements were performed on a Agilent Technologies 7890 A with FID (flame ionization detector) using a capillary column HP-5 (5% phenylmethylpolysiloxane) of 30 m length and 0.32 mm internal diameter as well as BP20(WAX) of 15 m length and 0.32 mm internal diameter as another column. Thereby, the samples were measured in high dilution using volatile organic solvents (usually ethanol or acetone).

### Nuclear magnetic resonance (NMR)

Liquid phase <sup>1</sup>H-NMR measurements were performed using a Bruker RMN AVANCE (AVANCE III) 300 MHz at 298 K and Bruker Avance DPX-200 spectrometer at 293 K in DCl/DMSO-d<sub>6</sub> for the digested activated MOF samples. Thereby, approximately 5 mg samples were digested in 4 droplets of DCl, placed in an ultrasonic bath for at least 30 min, and 0.7 mL DMSO-d<sub>6</sub> were added. For better digestion, the samples were carefully heated until the solution became clear.

## Acknowledgements

Funding by the Spanish Government is acknowledged through projects MAT2017-82288-C2-1-P and Severo Ochoa (SEV-2016-0683). This project is further funded by the Deutsche Forschungsgemeinschaft grant no. FI-502/32-1 ("DEMOFs"). KE and WRH would like to thank TUM Graduate School and the Gesellschaft Deutscher Chemiker (GDCh) for financial support. KE gratefully acknowledges support from the colleagues Olesia Halbherr (née Kozachuk) and Wenhua Zhang.

## Conflict of Interest

The authors declare no conflict of interest.

**Keywords:** Metal-Organic Frameworks · defects · ruthenium · Ru-BTC · Ru-MOF · HKUST-1 · Defect-Engineering · MOF catalysis · DEMOF

- [1] a) J. Gascon, A. Corma, F. Kapteijn, F. X. Llabrés i Xamena, *ACS Catal.* **2014**, *4*, 361–378; b) S. Hasegawa, S. Horike, R. Matsuda, S. Furukawa, K. Mochizuki, Y. Kinoshita, S. Kitagawa, *J. Am. Chem. Soc.* **2007**, *129*, 2607–2614; c) Z. Wang, S. M. Cohen, *Chem. Soc. Rev.* **2009**, *38*, 1315–1329.
- [2] a) F. Vermoortele, B. Bueken, G. Le Bars, B. Van de Voorde, M. Vandichel, K. Houthoofd, A. Vimont, M. Daturi, M. Waroquier, V. Van Speybroeck, C. Kirschhock, D. E. De Vos, *J. Am. Chem. Soc.* **2013**, *135*, 11465–11468; b) J. Zheng, J. Ye, M. A. Ortuño, J. L. Fulton, O. Y. Gutiérrez, D. M. Camaioni, R. K. Motkuri, Z. Li, T. E. Webber, B. L. Mehdi, N. D. Browning, R. L. Penn, O. K. Farha, J. T. Hupp, D. G. Truhlar, C. J. Cramer, J. A. Lercher, *J. Am. Chem. Soc.* **2019**, *141*, 9292–9304; c) S. M. J. Rogge, A. Bavykina, J. Hajek, H. Garcia, A. I. Olivos-Suarez, A. Sepúlveda-Escribano, A. Vimont, G. Clet, P. Bazin, F. Kapteijn, M. Daturi, E. V. Ramos-Fernandez, F. X. Llabrés i Xamena, V. Van Speybroeck, J. Gascon, *Chem. Soc. Rev.* **2017**, *46*, 3134–3184; d) D. Farrusseng, S. Aguado, C. Pinel, *Angew. Chem. Int. Ed.* **2009**, *48*, 7502–7513; e) P. Valvekens, F. Vermoortele, D. De Vos, *Catal. Sci. Technol.* **2013**, *3*, 1435–1445; f) C. J. Doonan, C. J. Sumbly, *CrystEngComm* **2017**, *19*, 4044–4048; g) A. Dhakshinamoorthy, Z. Li, H. Garcia, *Chem. Soc. Rev.* **2018**, *47*, 8134–8172; h) Y. Wang, C. Wöll, *Catal. Lett.* **2018**, *148*, 2201–2222; i) D. T. Genna, L. Y. Pfund, D. C. Samblanet, A. G. Wong-Foy, A. J. Matzger, M. S. Sanford, *ACS Catal.* **2016**, *6*, 3569–3574; j) H. Chen, Y. He, L. D. Pfefferle, W. H. Pu, Y. L. Wu, S. T. Qi, *ChemCatChem* **2018**, *10*, 2558–2570.
- [3] S. Marx, W. Kleist, J. Huang, M. Maciejewski, A. Baiker, *Dalton Trans.* **2010**, *39*, 3795–3798.
- [4] a) Z. Fang, B. Bueken, D. E. De Vos, R. A. Fischer, *Angew. Chem. Int. Ed.* **2015**, *54*, 7234–7254; b) S. Dissegna, K. Epp, W. R. Heinz, G. Kieslich, R. A. Fischer, *Adv. Mater.* **2018**, *30*, 1704501; c) Y.-B. Zhang, H. Furukawa, N. Ko, W. Nie, H. J. Park, S. Okajima, K. E. Cordova, H. Deng, J. Kim, O. M. Yaghi, *J. Am. Chem. Soc.* **2015**, *137*, 2641–2650; d) F. Drache, F. G. Cirujano, K. D. Nguyen, V. Bon, I. Senkovska, F. X. L. i Xamena, S. Kaskel, *Cryst. Growth Des.* **2018**, *18*, 5492–5500; e) W. Zhang, M. Kauer, O. Halbherr, K. Epp, P. H. Guo, M. I. Gonzalez, D. J. Xiao, C. Wiktor, F. Xamena, C. Woll, Y. M. Wang, M. Muhler, R. A. Fischer, *Chem. Eur. J.* **2016**, *22*, 14297–14307.
- [5] O. Kozachuk, K. Yusenko, H. Noei, Y. Wang, S. Walleck, T. Glaser, R. A. Fischer, *Chem. Commun.* **2011**, *47*, 8509–8511.
- [6] O. Kozachuk, I. Luz, F. X. L. i Xamena, H. Noei, M. Kauer, H. B. Albada, E. D. Bloch, B. Marler, Y. Wang, M. Muhler, R. A. Fischer, *Angew. Chem. Int. Ed.* **2014**, *53*, 7058–7062.
- [7] I. Agirrezabal-Tellería, I. Luz, M. A. Ortuño, M. A. Ortuno, M. Oregui-Bengoechea, I. Gandarias, N. Lopez, M. A. Lail, M. Soukri, *Nat. Commun.* **2019**, *10*, 2076.
- [8] a) W. Zhang, O. Kozachuk, R. Medishetty, A. Schneemann, R. Wagner, K. Khaletskaya, K. Epp, R. A. Fischer, *Eur. J. Inorg. Chem.* **2015**, 3913–3920; b) W. R. Heinz, T. Kratky, M. Drees, A. Wimmer, O. Tomanec, S. Gunther, M. Schuster, R. A. Fischer, *Dalton Trans.* **2019**, *48*, 12031–12039.
- [9] J.-E. Bäckvall, *J. Organomet. Chem.* **2002**, *652*, 105–111.
- [10] R. L. Chowdhury, J.-E. Bäckvall, *J. Chem. Soc. Chem. Commun.* **1991**, 1063–1064.
- [11] N. Ahlsten, A. Bartoszewicz, B. Martín-Matute, *Dalton Trans.* **2012**, *41*, 1660–1670.
- [12] a) N. Ahlsten, H. Lundberg, B. Martín-Matute, *Green Chem.* **2010**, *12*, 1628–1633; b) D. Cahard, S. Gaillard, J.-L. Renaud, *Tetrahedron Lett.* **2015**, *56*, 6159–6169; c) T. Xia, Z. Wei, B. Spiegelberg, H. J. Jiao, S. Hinze, J. G. de Vries, *Chem. Eur. J.* **2018**, *24*, 4043–4049; d) F. Scalambra, P. Lorenzo-Luis, I. de los Rios, A. Romerosa, *Coord. Chem. Rev.* **2019**, *393*, 118–148.
- [13] K. Yamaguchi, T. Koike, M. Kotani, M. Matsushita, S. Shinachi, N. Mizuno, *Chem. Eur. J.* **2005**, *11*, 6574–6582.
- [14] R. W. Mitchell, A. Spencer, G. Wilkinson, *J. Chem. Soc. Dalton Trans.* **1973**, 846–854.

Manuscript received: November 2, 2019

Revised manuscript received: January 19, 2020

Accepted manuscript online: January 23, 2020

Version of record online: February 19, 2020